Asia Pacific Academy of Science Pte. Ltd.

Eco Cities 2024, 5(2), 2818.
https://doi.org/10.54517/ec.v5i2.2818

Article

Impact of LULC spatial dynamics on incompatible mixed land use in Kaduna: A remote sensing and GIS risk analysis

Kamil Muhammad Kafi[1,2,3,*], Suraj Ibrahim[4,5], Fatima Umar Aliyu[3,6], Mashkurah Ahmed Usman[7], Kemi Hamdat Olugbodi[2]

[1] Department of Environment, Faculty of Forestry and Environment, Universiti Putra Malaysia, Serdang Selangor 43400, Malaysia
[2] Department of Urban and Regional Planning, Faculty of Earth and Environmental Sciences, Bayero University Kano, 700241, Nigeria
[3] Geospatial Research and Training Services Lab (GEORETS), Bauchi 702140, Nigeria
[4] Faculty of Management Sciences, Department of Business Management, Air Force institute Technology, Kaduna 800282, Nigeria
[5] Department of Information Management, School of Creative and Cultural Business, Robert Gordon University, Aberdeen AB10 7QB, United Kingdom
[6] Nigerian National Petroleum Corporation Limited, Kaduna 800282, Nigeria
[7] Department of Geography, Faculty of Social Science, Federal University of Kashere, Gombe 771103, Nigeria
*** Corresponding author:** Kamil Muhammad Kafi, kmkafi.urp@buk.edu.ng

CITATION

Kafi KM, Ibrahim S, Aliyu FU, et al. Impact of LULC spatial dynamics on incompatible mixed land use in Kaduna: A remote sensing and GIS risk analysis. Eco Cities. 2024; 5(2): 2818. https://doi.org/10.54517/ec.v5i2.2818

ARTICLE INFO

Received: 9 July 2024
Accepted: 27 August 2024
Available online: 10 September 2024

Abstract: This study assesses the spatio-temporal changes and the impact of urbanization leading to unchecked development within Kaduna city. By utilizing satellite remote sensing data and land use maps of Kaduna, the investigation focused on how the city has expanded over the years and the resultant spurring of incompatible land uses, where residential and commercial uses are increasingly mixed with industrial zones. Using LULC analysis, the results revealed that Kaduna has experienced a 145% increase in urban area between 2001–2014, with the expansion primarily occurring in the southern part of Kaduna metropolis. A change map showing different degrees of increase and decrease in land cover classes was obtained from the post-classification comparison. Using buffer analysis, the study identified and mapped risk zones that represent areas highly susceptible to adverse effects of industrial pollution in the study area. Notably, the Kakuri industrial area has seen significant new incompatible residential and commercial developments, and areas surrounding the Kaduna Refinery and Petrochemical Company (KRPC refinery) have witnessed the proliferation of high-density residential neighborhoods such as Sabon Tasha, Maraba, and Romi. Additionally, other areas such as Mando and Western Bypass are experiencing a mixture of industrial, residential, and commercial activities. These findings underscore the need for effective urban planning and land use management to address the challenges posed by rapid urban expansion and mixed land use in Kaduna.

Keywords: urban expansion; land use change; zoning; urban planning

1. Introduction

The dynamic nature of the urban environment does not always guarantee safety for its inhabitants. Human activities within their immediate environment bring about certain changes in the Land Use Land Cover (LULC) patterns over time [1–3]. Consequently, if these changes are not continuously monitored, they can lead to negative impacts that affect both the environment and its inhabitants [4]. Kaduna, the former administrative center of the northern states of Nigeria, is one of the urbanizing cities in the country and has witnessed tremendous expansion in recent decades [5,6]. This expansion is primarily due to an increase in population and developmental activities related to land and buildings over the last few decades [7]. It is widely agreed

that a deeper understanding of urban expansion is essential for the effective and sustainable use of land resources [8].

Urbanization often leads to the proliferation of both organic and compact neighborhoods, driven by the influx of people seeking better economic opportunities and living conditions [9–11]. As cities expand rapidly, some developments tend to digress from the original master plan, resulting in the emergence of incompatible land uses adjoining each other [12,13]. Residential areas may develop adjacent to industrial zones, commercial establishments may sprout in previously residential districts, and informal settlements may encroach upon planned urban spaces. This haphazard growth creates spatial hazards such as increased pollution, traffic congestion, and heightened risk of industrial accidents affecting residential communities [14–16]. The lack of cohesive urban planning exacerbates these issues, as the infrastructure and services in these mixed-use areas often lag behind, leading to suboptimal living conditions and potential health and safety risks for the inhabitants [17–19]. Therefore, managing urbanization through development control and spatio-temporal monitoring of urban land use change is crucial to ensure meaningful, healthy, and sustainable development [20–22].

Additionally, the connection between land use and ecological development is crucial, as changes in LULC directly impact environmental sustainability. Urban expansion and alterations in land cover can disrupt ecosystems, influence hydrological cycles, and exacerbate natural hazards like floods [23]. Therefore, investigating the interplay between land use dynamics and ecological development is vital for informed decision-making in urban planning and environmental management.

There are various approaches to spatio-temporal monitoring of urban LULC and assessing its multi-dimensional impacts, including AI-based machine learning and deep learning techniques, geospatial methods using multi-date image processing, and data analytics through statistical modeling and trend analysis [4,21,24]. These methods have been widely employed and proven effective in understanding the pattern and dynamics of urban expansion. For example, Wang et al. [25] explored various machine learning models, comparing their strengths in modeling and predicting LULC changes. Hyandye et al. [26] examined the impact of urban growth and climate change on water availability in Tanzania using a geospatial approach, concluding that both LULC changes and climate variations significantly influence hydrological processes within the watershed. Similarly, Singh et al. [27] employed satellite data and machine learning techniques to model LULC changes in India, reporting high prediction accuracies. In another study, Nkiruka et al. [23] used a geospatial approach based on remote sensing and GIS tools to assess how LULC changes in Onitsha, Nigeria, exacerbate flood exposure.

Therefore, obtaining accurate and up-to-date information on land cover changes is essential for understanding and assessing the environmental consequences of such changes [28]. Satellite remote-sensing techniques have been widely employed to detect and monitor land cover changes at various scales, yielding valuable results [29,30]. Remote sensing has the capability to capture these changes; however, extracting the change information from satellite data requires effective and automated change detection techniques [31]. It is imperative to consistently monitor these changes so that planners and policymakers can evaluate the impacts of land use

transitions and propose alternative land use strategies for development purposes [20].

The objective of this research is to utilize geospatial technologies to assess the magnitude of spatial change and the impact of LULC conversion on land use compatibility over a period of 13 years. By employing remote sensing and GIS tools [32–34], this study aims to provide a detailed analysis of urban expansion and its consequences on the spatial organization of Kaduna. By mapping these risk areas, the research intends to offer valuable insights for urban planners and policymakers, enabling them to devise strategic interventions that promote harmonious land use, mitigate potential hazards, and ensure sustainable urban development.

2. Materials and methods

2.1. Study area

Kaduna is a new town founded in 1917 during the second decade of British rule in Nigeria. Kaduna is unique amongst Nigerian major cities. The Kaduna metropolis is situated in between latitudes 10°36′ N and 11°6′ N and longitudes 7°23′ E and 7°31′ E [35,36]. Its establishment brought to an end the protracted search for a suitable administrative seat/capital for northern Nigeria [37]. Kaduna regional topography consists of a rolling part-like tracing with little relief situated about 100 feet above and below in broad, shallow valleys separated by conspicuous water sheds.

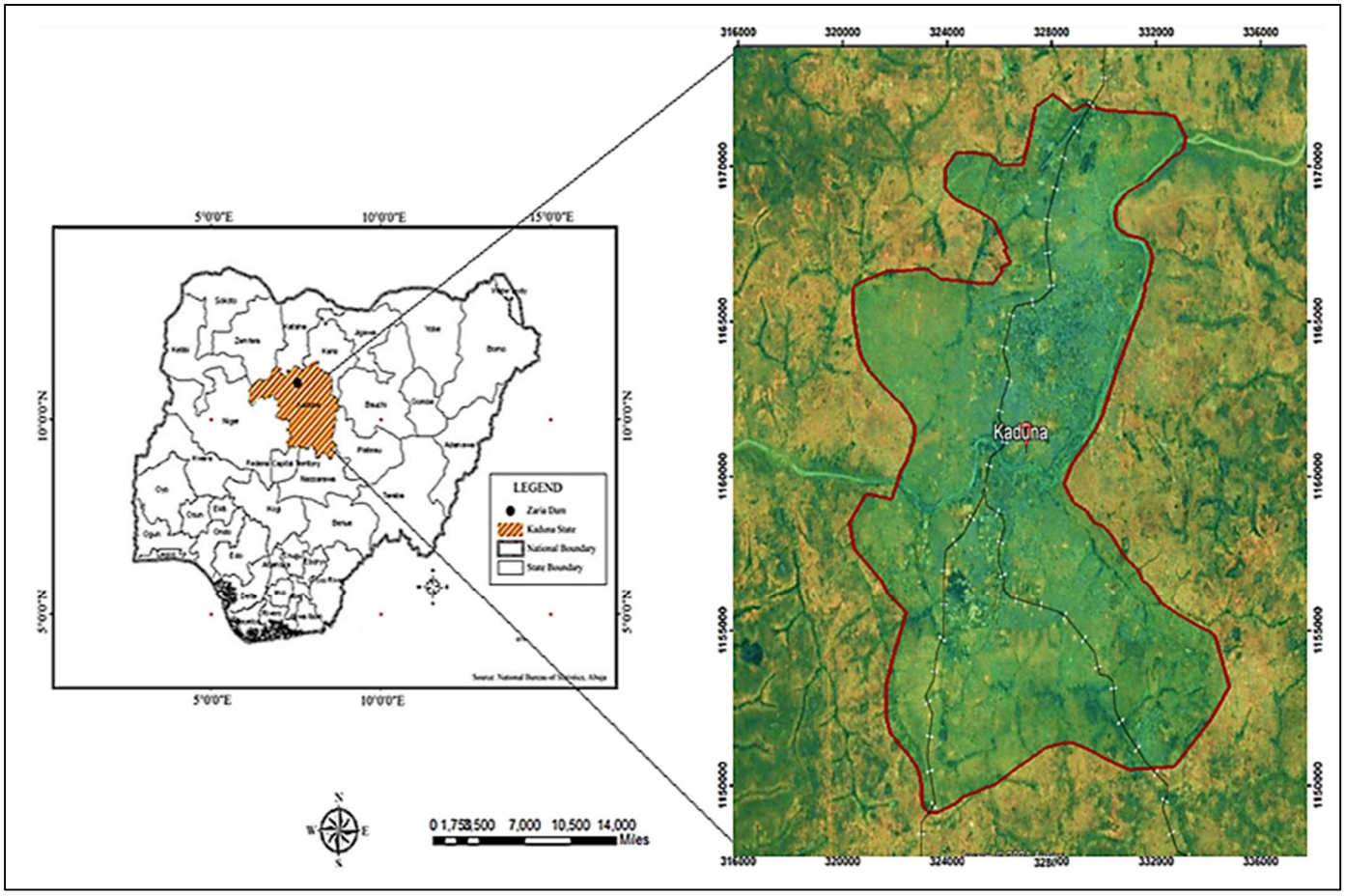

Figure 1. Showing Kaduna metropolitan area.

Kaduna is situated within the Northern Guinea savannah zone (see **Figure 1**). This, however, implies woodland vegetation is characterized by the presence of shrubs and trees. A study of vegetation within Kaduna metropolis carried out by Al Amin and Dadan [38] reveals the presence of certain tree species, such as *Mangifera indica* (Mango), *Duranta* spp., *Casuarina* spp., and *Delonix regia* (Flamboyant tree), which are the dominant tree species found within the city.

2.2. LULC classification

Using a supervised classification technique, the study categorized and grouped LULC types into five distinct classes, accounting for all significant LULC types within the study area [33]. These classes include built-up areas, vegetation cover, water bodies, bare land, and other land types. The built-up area category encompasses all man-made structures such as road networks, industries, low, medium, and high residential areas, as well as dispersed settlements on the outskirts of the city. The vegetation cover class includes all types of vegetation canopy covering the top layer of the soil, such as agricultural crops, trees, shrubs, and grasses. The water body class consists of rivers, ponds, and other waterlogged areas. The bare land category refers to portions of land that are unused and exposed to direct sunlight. Finally, the other land category includes rock outcrops and ditches.

Additionally, the study utilized GIS tools to identify risk zones for industrial pollution based on factors like proximity to incompatible land uses, prevailing wind direction, and buffer zones. Using multiple ring buffer analyses, distances of 500 m, 300 m, and 200 m were assigned to industrial effluents, with areas within these buffers considered vulnerable to pollution. Additionally, land uses downwind within 1 km of industrial areas were deemed susceptible to air pollution. Areas lacking buffer zones to mitigate noise and air pollution were also identified as risk zones. This methodology provides a comprehensive assessment of areas vulnerable to industrial pollution, aiding urban planning and environmental management in Kaduna.

2.3. Data acquisition

The study utilized satellite imageries from Landsat to process and monitor LULC changes in Kaduna city from 2001 to 2014 [39,40]. The satellite data used in this study were acquired from two different sensors at two different times of the season. The first image was captured by Landsat 7 ETM + in October 2001, during the rainy season when vegetation cover is typically at its peak. The second image was acquired by Landsat 8 in February 2014, during the dry season when vegetation cover is usually minimal. Before data acquisition, both images were meticulously examined to ensure that they had less than 20% cloud coverage, thus providing clear and accurate data for analysis [21]. In addition to satellite imagery, the study also utilized historical land use data, including the master plan of 1967 for Kaduna [41]. This master plan provided a comprehensive overview of the intended land use allocations of the city.

2.4. Pre-processing

2.4.1. Radiometric calibration

Handling satellite images for analysis of any kind requires radiometric calibration

in order to allow for the extraction of information based on reflectance and not just radiance. Any quantitative analysis involving two or more satellite images needs to be adjusted radiometrically to compensate for the difference in whether, time variation, and illumination amongst the dataset [42]. To achieve a meaningful urban land cover change detection analysis based on a satellite image, the radiometric response must be obtained [43,44]. The quantification of change using a multitemporal image is difficult to interpret without performing the radiometric correction [45]. Ultimately, there are three ways of restoring the radiometric response on Landsat images [46]. The procedure of radiometric calibration involves converting the image into (1) radiance, (2) Top of Atmospheric (TOA) reflectance, and (3) brightness temperature (USGS, 2024).

Conversion to radiance

This is the fundamental step in enhancing the radiometric quality of a satellite image. This step involves the conversion of pixel values (Q) from unprocessed image data into a unit of absolute spectral radiance using 32-bit floating point calculations. While the absolute radiance is scaled to 16, 8, or 7-bits depending on the sensor's radiometric resolution [45,46].

$$\left(L_\lambda \frac{(L_{\max\lambda} - L_{\min\lambda})}{Q_{\text{calmax}} - Q_{\text{calmin}}}\right) \times (Q_{\text{cal}} - Q_{\text{calmin}}) + L_{\min\lambda}$$

where:

L_λ = Cell value as radiance.

Q_{cal} = Digital Number.

$L_{\min\lambda}$ = Spectral Radiance scale to Q_{calmin}.

$L_{\max\lambda}$ = Spectral Radiance scale to Q_{calmax}.

Q_{calmin} = Minimum quantized calibrated pixel value (typically = 1).

Q_{calmax} = Maximum quantized calibrated pixel value (typically = 255).

Conversion to TOA reflectance

Conversion to TOA is done to correct for the variation in earth's sun distance between data acquired on different dates. These variations could be in 1) distance, (2) solar irradiance due to band difference, and (3) solar zenith angle due to difference in time of the day [45]. TOA reflectance can be computed using the equation [46].

$$p_\lambda = \frac{\pi L_\lambda d^2}{\text{ESUN}_\lambda \sin\theta}$$

where:

p =Unitless planetary reflectance (the ration of reflected versus total power energy).

L_λ = Spectral radiance at sensor's aperture (at-sensor radiance).

d^2 = Earth–Sun distance in astronomical units.

ESUN_λ = Mean solar exo-atmospheric irradiance.

sin θ = Solar zenith angle in degrees.

Conversion to at-sensor brightness temperature

The at-sensor brightness temperature is converted using the thermal band by assuming the earth surface is a black body, i.e., having emissivity equal 1, which also includes absorption and emission along the path. The thermal constant is provided in

the image metadata file and can be computed using the equation below [46].

$$T = \frac{K_2}{\ln\left(\frac{K_1}{L_\lambda} + 1\right)}$$

where:

T = At-sensor brightness temperature in Kelvin (K).

L_λ = TOA spectral radiance (Watts/(m^2 * srad * μm))

K_1 = The calibration constant 666.09 in Watts/(m^2 * sr * μm)

K_2 = The calibration constant 1282.71 in degrees Kelvin

2.4.2. Atmospheric correction

Satellite imagery can be influenced by various atmospheric factors depending on the time of year and season. These factors introduce distortions in the imagery, affecting how the Earth's surface is depicted [47,48]. One significant factor is the variation in illumination due to changes in the angle of the sun relative to the Earth's surface, occasioned by different seasons or times of day. Similarly, the two images acquired for this study were not only acquired in different years but also at different seasons of the year. The first image was acquired during the rainy season, while the second image was acquired during the dry season; this accounts for the illumination difference and the atmospheric effects prevalent on the images. To correct these effects, the atmospheric correction was performed with ENVI 5.1. First, the images were calibrated to radiance and reflectance using the MTL Multispectral dataset and then calibrated to brightness temperature using the thermal band with the scale factor set at 1, using the original unit of the data to ensure accurate brightness temperature measurements. Similarly, the FLAASH atmospheric correction was performed also using the MTL file. The initial visibility was set to 40 km by default, which indicates clear atmospheric conditions throughout the scene. Finally, the FLAASH atmospheric result was validated using the spectral profile.

2.5. Landsat band combinations

The choice of an appropriate band combination for an RGB image is essential for any kind of digital image processing and analysis. Selecting three different bands to create color imagery is crucial for accurately identifying and analyzing land cover features. For the purpose of this study, the guide by Horning [49] was very helpful in selecting the appropriate band combinations. In **Figure 2(A1–C1)**, the band combinations are as follows: A1 is a False Color Composite (FCC) best for identifying vegetation and water, B1 is an FCC best for urban areas, and C1 is an FCC best for bare land. In **Figure 2(A2–C2)**, the band combinations are: A2 is an FCC best for urban areas, B2 is an FCC best for bare land, and C2 is an FCC best for vegetation. These combinations were used to enhance the visualization and differentiation of various land cover types in the study area, facilitating accurate analysis and interpretation.

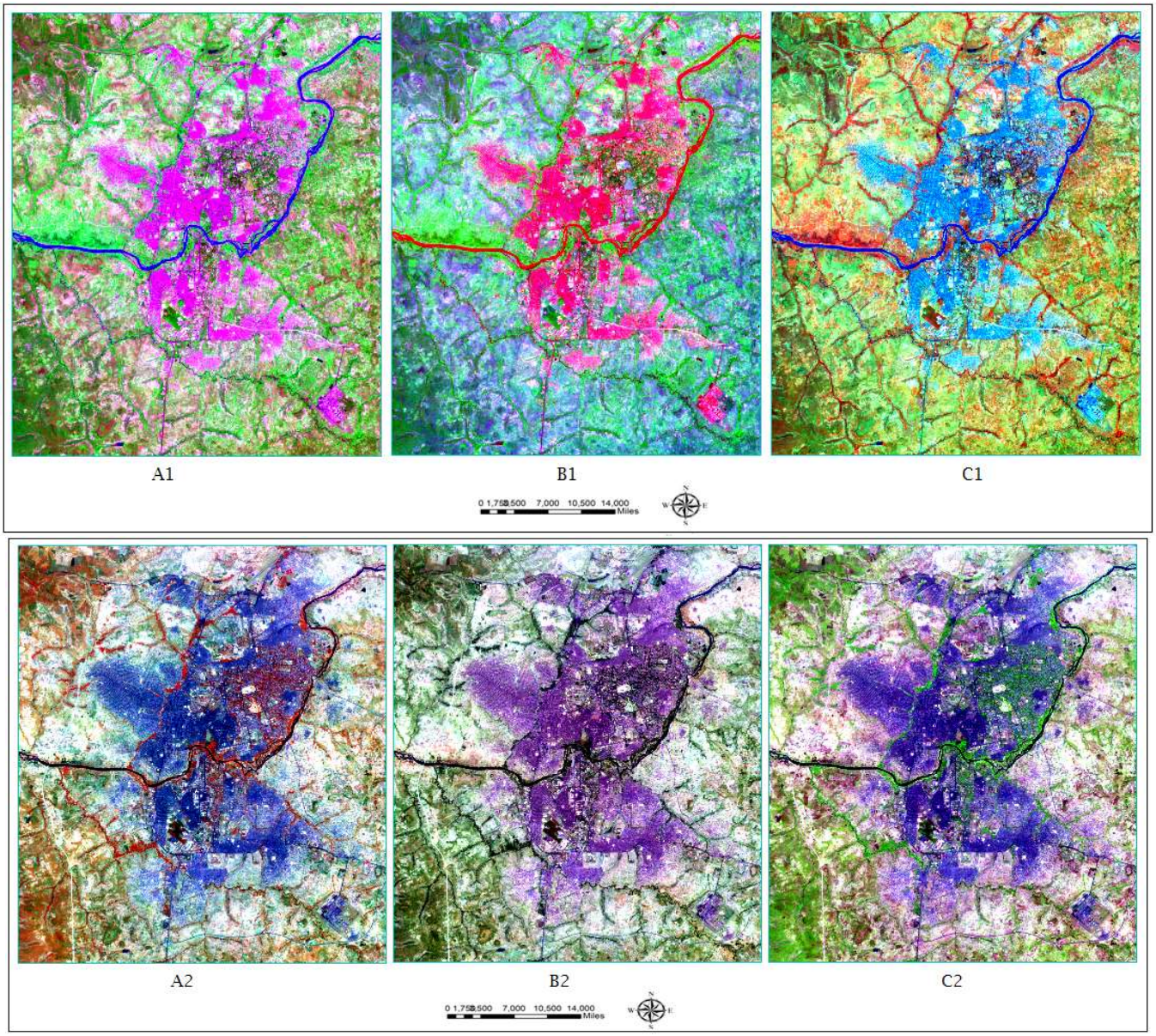

Figure 2. (A1–C1) Landsat 7 false color composite; **(A2–C2)** Landsat 8 false color composite for the identification of certain LULC features (Adopted from Horning (2004)).

RGB combination: A1 = 5, 4, 3; B1 = 1, 4, 5; C1 = 4, 5, 1.
RGB combination: A2 = 7, 6, 4; B2 = 5, 6, 4; C2 = 6, 5, 4.

2.6. Image classification

2.6.1. Image differencing

This technique is performed by comparing two different images from two different datasets using either the band ratio or feature index technique. The difference in the areas of change will have positive or negative values, while areas of no change will have a zero value [50]. In this study, the image differencing technique was carried out in ENVI 5.1 to produce a difference change map from the two satellite imageries. The feature index technique could not be performed due to the difference in satellite band numbers and composition. The image differencing using this technique can only be carried out for change detection analysis using two different images from the same

sensor. Furthermore, applying the band ratio technique did not yield any meaningful results since only the image difference of one band at a time can be presented as the output map.

2.6.2. Supervised classification

This algorithm has been found to be among the most effective approaches to LULC assessment and evaluation [20]. This algorithm is categorized into three stages: (1) training stage, (2) classification stage, and (3) output stage (Lillesand and Kiefer, 2008). The supervised classification approach was carried out using the maximum likelihood classifier. Before assigning the Region of Interest (ROI), the application of false color composites aided in extracting more information about some of the land cover features because some features are best identified using the false color composite (see **Figure 2A–C**). This classification yielded the best result for the two date images, with an overall accuracy of 94.88% and a Kappa coefficient of 0.83 for the first date image, while an overall accuracy of 85.18% and a Kappa coefficient of 0.79 were obtained for the 2014 map.

2.7. Post-classification

The main aim of LULC change detection is to produce a from-to-change map product from the two independently classified images. In this study, this comparison technique was carried out using the two different dates' maps to produce the final change map. A positive pixel value above zero indicates an increase in the land cover, a zero-pixel value indicates no change, and a negative pixel value indicates a decrease in the land cover. Finally, the post-classification comparison was very effective because it presents a three-class map, i.e., increase change, no change, and decrease change through pixel-by-pixel comparison.

2.8. Accuracy assessment

Accuracy assessment is a necessary component of any digital change detection analysis because its product represents how well the LULC analysis reflects the true land cover. The accuracy of the two classified maps was assessed and presented in an error matrix. For this purpose, two different sets of data (ROI) were used. The first set of ROIs was used to train the pixels for generating the digital map, while the second set of ROIs was used as testing data for generating the confusion matrix. This was done to avoid possible bias in the analysis process [4]. The distribution of the ROIs throughout the images increased the chances of the training data being a true representation of all the variations in the land cover classes presented in the map. This is because there is a positive correlation between the size and distribution of training sites and the accuracy of the classification [51].

3. Results

The derived LULC maps for the two different dates have been compared and analyzed based on the results of the error matrix and the differences exhibited in the spatial pattern of each of the product maps. A comparison of the two maps reveals a significant 122.9% increase in built-up areas, while land cover types such as vegetation, bare land, and water bodies have inevitably decreased, with 50%, 49.4%,

and 10.4%, respectively, being converted to built-up areas (see **Figure 3**).

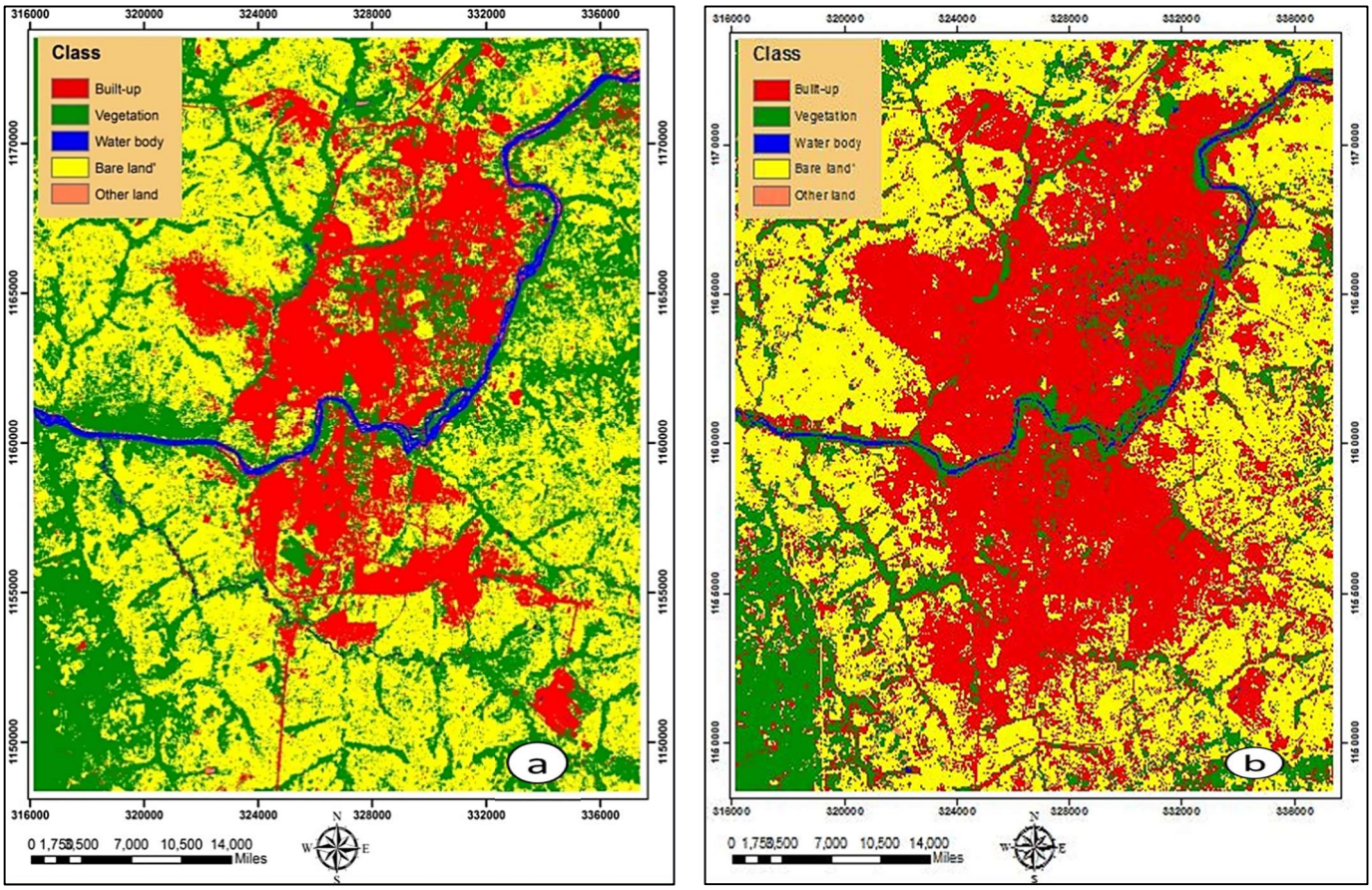

Figure 3. Showing **(a)** 2001; and **(b)** 2014 LULC classes of Kaduna based on supervised technique.

3.1. LULC change detection

3.1.1. Built-up

The built-up area has witnessed a significant increase over the study period. The analysis revealed a tremendous growth in the built-up land cover class from an initial size of 99.1 km^2 (18.5% of total area in 2001) to a surprising 209.8 km^2, constituting 41% of the total land area in 2014. This high level of increase is due to the collective efforts of the government, private organizations, and individuals in developing the city. As the administrative center of all the northern states in Nigeria, Kaduna sees daily construction of building structures of all types and purposes to support the increasing demand for housing, business, and workplaces.

The accuracy assessment for the two classified maps reveals distinct differences in the user and Kappa accuracies for the years 2001 and 2014, both of which fall within the minimum acceptable value of 85% [20]. The 2001 classification achieved high producer and user accuracy for all classes, with water body attaining the highest accuracy as no pixel was misclassified. The overall accuracy for 2001 was 94.88%, with a Kappa coefficient of 0.83, indicating a high level of agreement between the classified map and the reference data. In contrast, the 2014 classification exhibited some reduction in accuracy. While it maintained a good overall accuracy of 85.18% and a Kappa coefficient of 0.79, several classes had lower producer and user

accuracies (see **Tables 1** and **2**). This decrease is attributed to the heterogeneous nature of the urban area, which led to some misclassification of the ROI pixels. For example, the proliferation of mixed land use, varying roofing materials, diverse infrastructure, and a wide range of activities contribute to the heterogenous and diverse urban form and structure of Kaduna [52,53]. These subtle and intricate patterns make it challenging to achieve very high accuracy of land cover classification, particularly when using low spatial resolution data [54].

Table 1. Error Matrix table derived from 2001 satellite data.

	Built-up	**Vegetation**	**Water Body**	**Bear Land**	**Other Land**	**Prod. Acc. (%)**	**User Acc. (%)**
Built-up	1417	0	0	1	1	99.4	94.53
Vegetation	0	96	0	0	0	98.97	100
Water Body	0	0	33	0	0	100	100
Bear Land	8	1	0	135	0	99.26	93.75
Other Land	0	0	0	0	7	7.95	93.75
Total	1425	97	33	136	88		
Overall Accuracy:	94.88%	Kappa Coefficient: 0.83					

Table 2. Error Matrix table derived from 2014 satellite data.

Class	**Built-up**	**Vegetation**	**Water**	**Bare land**	**Other land**	**Acc. (%)**	**Acc. (%)**
Built-up	150	28	0	39	7	97.4	66.96
Vegetation	3	428	17	0	0	81.37	95.54
Water Body	0	0	274	0	4	94.16	98.56
Bear Land	1	70	0	120	0	75.47	62.83
Other Land	0	0	0	0	0	00.0	00.0
Total	154	526	291	159	11		
Overall Accuracy: 85.18%		Kappa Coefficient: 0.79					

3.1.2. Vegetation

The vegetation cover in Kaduna city has experienced a drastic decrease from 193.0 km^2, constituting 36.1% of the total land in 2001, to 96.5 km^2, equivalent to 18.1% of the total land area in 2014 (see **Table 3**). The highest amount of conversion was to bare land. This is due to the difference in the time of data acquisition between the first and the second image. The 2001 image was acquired during the rainy season, a period characterized by increased shrubs, grasses, and agricultural farming practices, while the 2014 image was acquired during the dry season. Since Kaduna is a semi-arid area, most of its vegetation cover, such as shrubs and grasses, tends to dry up during the dry season. Similarly, the agricultural crops are mostly annual crops planted during the rainy season and harvested during the dry season. Additionally, a significant proportion of the vegetation was converted to built-up areas due to the increased demand for housing, construction of roads, and other man-made structures.

Table 3. Percentage and magnitude of change between 2001–2014.

Class	2001		2014		Change magnitude	Total Change
	(km^2)	(%)	(km^2)	(%)	(km^2)	(%)
Built-up	99.1	18.5	220.9	41.2	121.8	122.9
Vegetation	193.0	36.1	96.5	18.1	−96.5	50
Water body	8.3	1.5	4.1	0.7	−4.1	49.4
Bare land	234.1	43.7	209.8	39.2	−24.4	10.4
Other land	0.8	0.2	4.0	0.7	3.2	400
Total	535.3	100	535.3	100		

3.1.3. Water body

The study revealed a decrease in the total area identified as water bodies, from 8.3 km^2 in 2001 to 4.1 km^2, now standing at 0.7% of the total land area under study. This decrease is primarily due to the variation in the data acquisition seasons. Some shallow valleys that were waterlogged and identified as water bodies in the 2001 image have dried up and converted to bare land. Others, where moisture content is retained, have grown grasses and shrubs, thereby being identified as vegetation. Additionally, some portions of the water bodies were sand-filled and converted to built-up areas.

3.1.4. Bare land

Bare land comprises only the exposed surface of the topsoil found within the study area. Over the years, the study has revealed a decrease in this category. Bare land, which had the highest proportion and percentage of land area in the first date with a total coverage of 234.1 km^2, equivalent to 43.7%, has been reduced to 209.8 km^2, constituting 39.2% in 2014 (see **Table 3**). This reduction can be attributed to the increased demand for urban land use, which inevitably led to some portions of the bare land being converted to built-up areas. Although a significant proportion of the bare land has been taken over by built-up areas, the overall decrease in bare land is considered small proportionately. The seasonal variation that saw a greater proportion of vegetation converted to bare land played a major role in preventing a significant decrease in the total area covered by bare land.

3.1.5. Other land

During the study period, the area categorized as "other land" has increased over the years. However, bare land pixels have been mixed with some of the other classes, revealing a complete conversion of the initial land area to the rest of the classes. This increase is partly due to the misclassification of bare land pixels (see **Table 3**).

3.2. Post-classification comparison

The first and second classified maps were compared on a pixel-by-pixel basis for each land cover class (see **Figure 4a,b**). The final output change map, shown in **Figure 4a**, was presented in three different colors, representing (1) an increase in change, (2) no change, and (3) a decrease in change. The increase and decrease in change were presented based on the magnitude of change that has taken place.

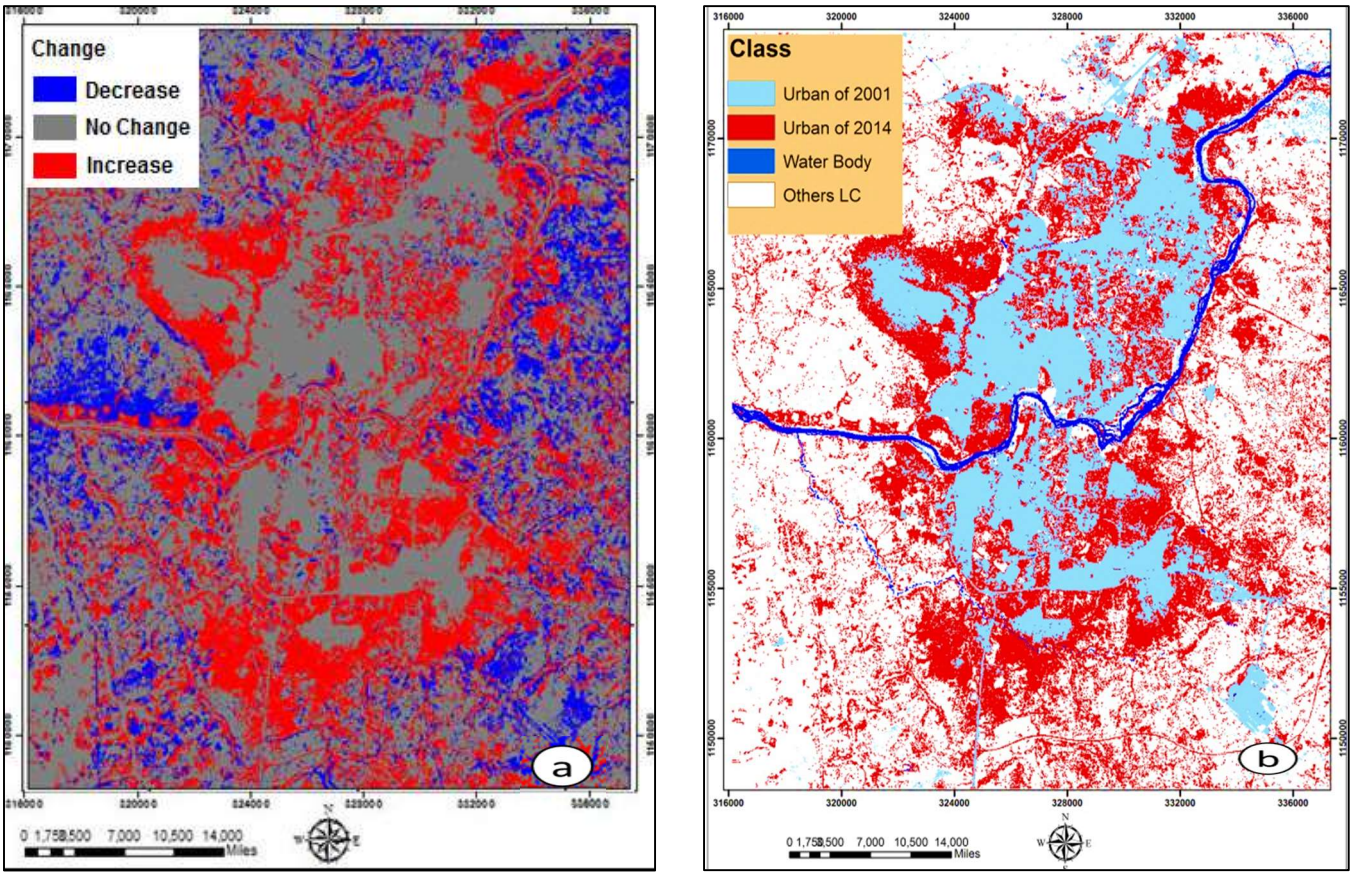

Figure 4. (a) Spatial change based on increase or decrease; **(b)** showing the extent of built-up expansion during the study period.

3.3. Urban expansion and its impacts

3.3.1. Spatial development

Spatially, the expansion of Kaduna's built-up area has been evident in both its northern and southern regions. The establishment of KRPC refineries and other industrial establishments in the south has driven rapid development, attracting a significant influx of immigrants. This concentration of industries along the southern banks of the Kaduna River solidifies the city's position as Nigeria's fifth-largest. Additionally, the development of the northern part of the city was triggered by the construction of the western expressway linking five major cities, including the Federal Capital Territory of Nigeria, a few decades ago. However, the expansion of the city around the eastern part has been hindered by the lack of access bridges over the Kaduna River. Nonetheless, the recent construction of the new Makarfi Bridge and the ongoing plan for a new Kaduna city suggest potential growth in this area.

The result of the from-to changes that have taken place over the period of study is shown in **Table 4**. Each of the land cover classes has experienced a class change, i.e., conversion to another LULC class. Ultimately, the biggest from-to change that has taken place over the period is 78.6 km^2, which constituted a 33.6% increase in built-up. Meanwhile, the smallest from-to change is 0.1 km^2 but has repeatedly occurred amongst three different land cover classes, from built up to other land, other land to bare land, and from other land to water bodies.

Table 4. Area and percentage of spatial conversion of LULC classes between 2001–2014.

Change from	Change to	Change (km^2)	Change (%)
Built up	Vegetation	4.2	4.3
	Water Body	0.4	0.4
	Bare Land	5.1	5.2
	Other Land	0.1	0.1
Vegetation	Built up	51.5	26.7
	Water Body	0.2	0.1
	Bare Land	66.4	34.4
	Other Land	2.3	1.2
Water Body	Built up	1.3	15.8
	Vegetation	3.6	43.6
	Bare Land	0.03	0.3
	Other Land	0.0	0.0
Bare Land	Built up	78.6	33.6
	Vegetation	15.7	6.7
	Water Body	0.0	0.0
	Other Land	1.6	0.7
Other Land	Built up	0.3	35.6
	Vegetation	0.4	46.5
	Water Body	0.1	10.8
	Bare Land	0.1	7.1

3.3.2. Land use incompatibility

The rapid expansion of metropolitan Kaduna has resulted in the emergence of incompatible land uses, as shown in **Figure 5a,b**. For example, the Kakuri industrial layout, carefully designated in the original master plan, has experienced de-industrialization, with commercial activities encroaching alongside the emergence of residential developments. Moreover, while the KRPC refinery is located at a distance from metropolitan Kaduna, it has stimulated rapid development in new neighborhoods such as Sabon Tasha, Kamanzo, Maraba, and Romi. Despite this growth, these developments are incongruent with the intended purpose of the KRPC refinery's industrial estate (see **Figure 5a,b**). Furthermore, the Mando axis has also seen industrial developments emerge within the mix of commercial activities. Overall, these developments highlight the need for careful urban planning to ensure sustainable and compatible land use in Kaduna's expanding urban landscape.

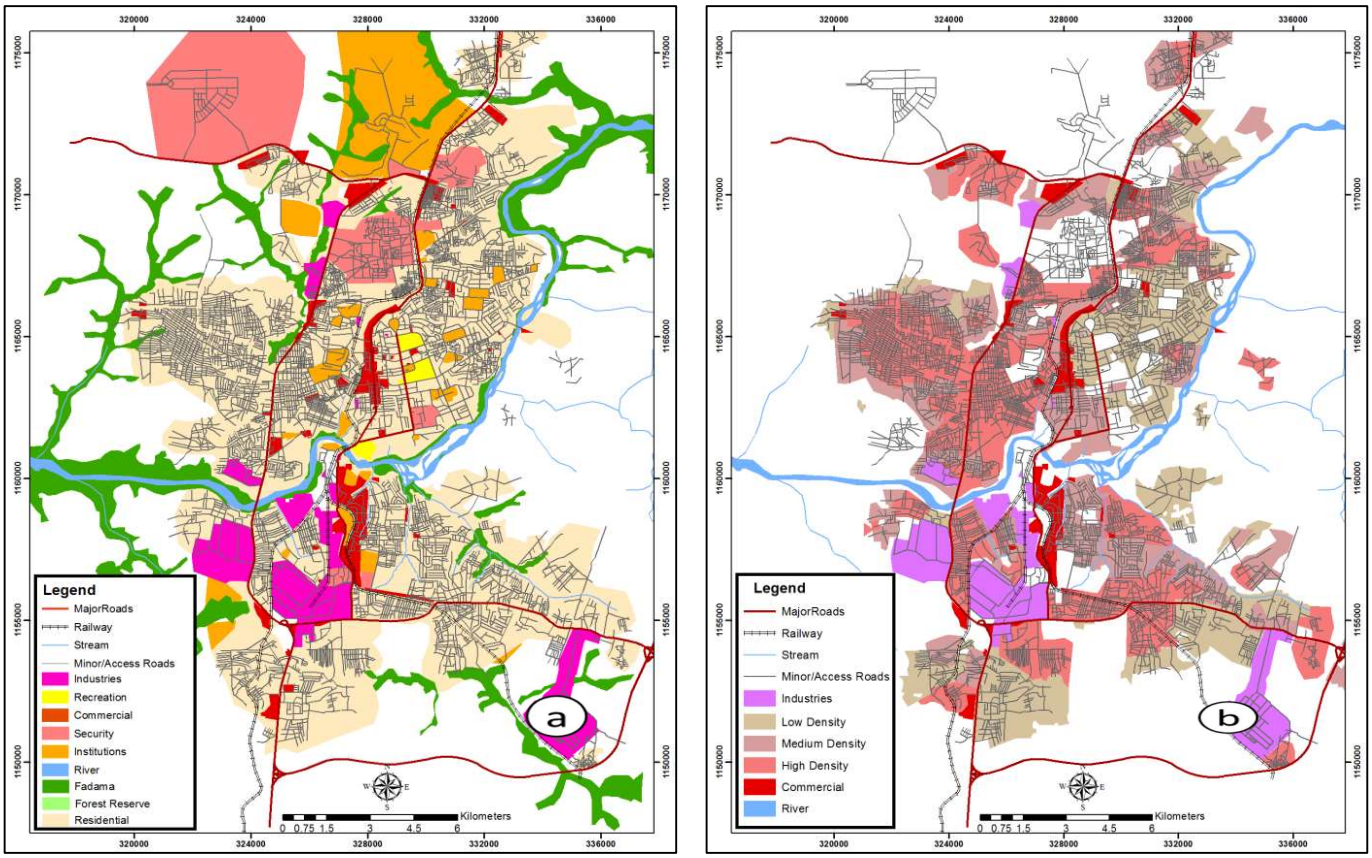

Figure 5. (a) Land use map of metropolitan Kaduna; **(b)** residential density map of Kaduna, modified from the data obtained from EDRES Consultants (2014).

3.3.3. At-risk zones

For the purpose of mapping risk areas, a multiple ring buffer analysis was conducted based on distances of 500 m, 300 m, and 200 m, depending on the type of industrial activities and anticipated pollution impact, as identified in the study. The 500 m, 300 m, and 200 m setbacks are aligned with the minimum standards set by the Kaduna State Urban Development Agency (KASUBDA) for different types of industries. These distances are based on considerations related to emissions, effluents, and the noise and vibrational effects from industrial equipment and processing [55–57]. Risk zones represent areas highly susceptible to the adverse effects of industrial pollution and poor air quality in the study area [16,58,59]. These zones were identified based on their proximity to industrial facilities lacking buffer zones and exposure to prevailing wind patterns. The highlighted regions indicate zones where industrial activities encroach upon residential neighborhoods and commercial establishments, posing potential hazards such as air and noise pollution and other environmental risks (see **Figure 6**). Neighborhoods mapped as high-risk areas are especially those within the Kakuri industrial layout, identified as risk zones using a 500 m buffer. Next are the risk zones adjoining the KRPC refinery, followed by those in Mando or the northern axis of Kaduna. The identification of risk zones serves as a crucial step in urban planning and environmental management, highlighting areas requiring immediate attention and targeted intervention to mitigate the negative impacts of industrial activities on public health and the environment. By delineating these zones,

policymakers and stakeholders can implement measures to enhance pollution control, improve infrastructure resilience, and safeguard the well-being of communities in Kaduna.

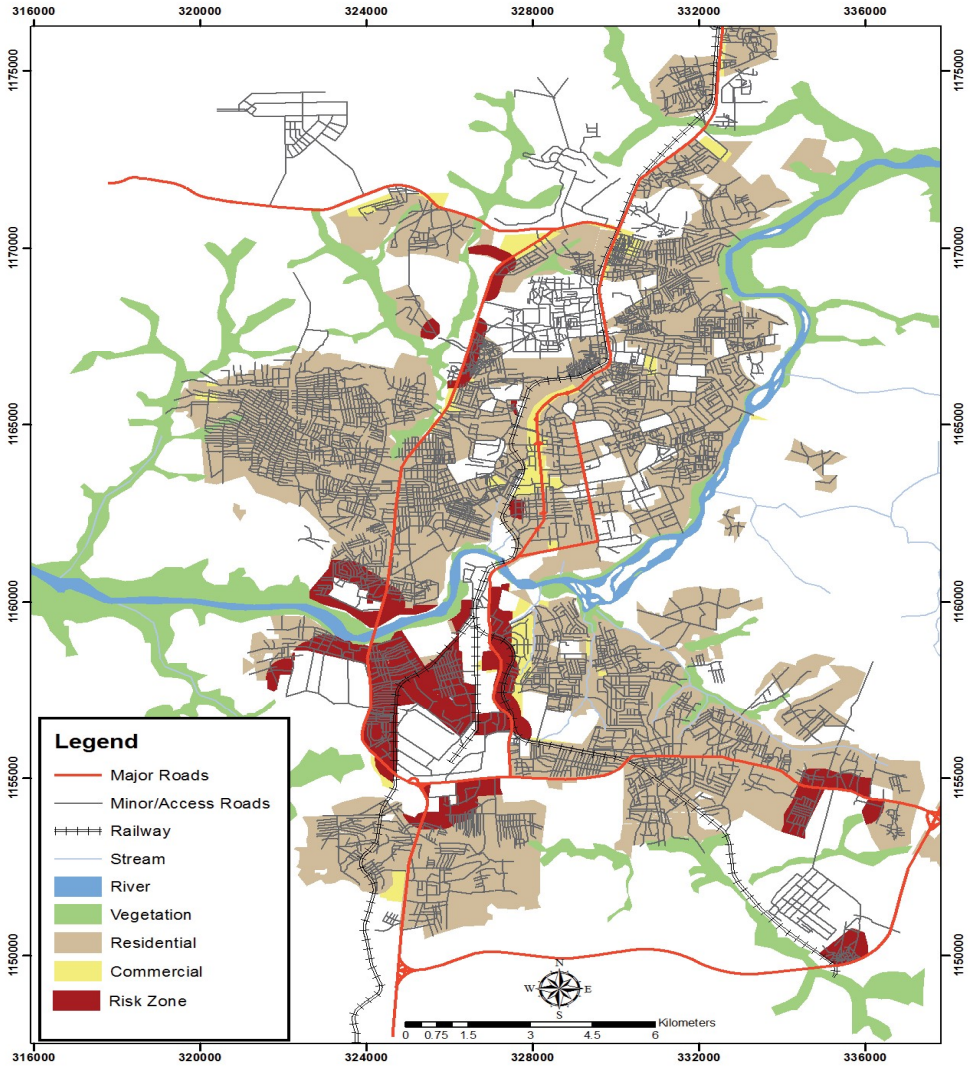

Figure 6. Risk areas based on land use incompatibility between industrial, residential, and commercial activities.

4. Discussion

The rapid urban expansion in Kaduna has led to significant land use and land cover (LULC) changes, resulting in the development of incompatible mixed uses. The transformation of open land and designated industrial buffers into residential and commercial areas has disrupted the planned urban structure, leading to various challenges and inefficiencies. One of the most noticeable changes is the mixing of residential developments into areas originally intended as industrial layouts, including buffer areas. These open lands were designated to act as separation zones, mitigating the impact of industrial activities on residential areas. However, the increasing demand for housing has led to these buffers being overtaken by residential developments. This encroachment not only compromises the safety and well-being of residents due to proximity to industrial operations but also disrupts the intended urban planning.

Another significant issue arising from the rapid urbanization in Kaduna is the emergence of commercial activities within industrial settings. Originally planned industrial areas are now interspersed with commercial establishments, such as shops and offices. This mixture creates a complex urban environment where industrial operations coexist with commercial activities, leading to increased traffic congestion, noise pollution, and safety hazards [60]. The lack of clear zoning and regulatory enforcement exacerbates these issues, making it difficult to maintain orderly urban development. Therefore, achieving city-wide sustainable urban development requires the integration of spatial planning, policy decisions on development control and zoning regulations, and inclusive community engagement and awareness on hazard prevention [18,61,62].

The uncontrolled urban sprawl has also necessitated the emergence of light and heavy industries outside the designated industrial layouts in Kaduna [63]. As industrial zones become saturated and land availability diminishes, new industries are established in areas originally zoned for residential or other uses, and vice versa [64]. This unplanned industrial expansion therefore creates several environmental concerns [65,66]. The proximity of industrial facilities to residential areas poses health and safety risks to inhabitants due to potential exposure to industrial emissions and accidents [67]. For example, a study by Emigilati et al. [68] revealed that the close proximity of residential buildings to the Kakuri Industrial Estate in Kaduna has led to significant pollution and health problems. Because the discharge of industrial effluents, combined with municipal waste, has resulted in severe contamination of river water, posing serious environmental and public health risks. Additionally, the development of some industries outside the designated areas often lacks the desirable buffer zone needed to filter and clean polluted air from industrial processes before it reaches neighboring residential and commercial areas. Additionally, these industries often lack proper infrastructure for waste management, leading to pollution and environmental degradation. The mixing of industrial and other land uses also strains existing infrastructure—such as roads, water supply, and electricity—which were not designed to support industrial operations, invariably affecting urban livability [60,63,69,70].

5. Conclusion

The study revealed a remarkable surge in urban expansion, notably seen in the substantial growth of built-up areas. Starting at 99.1 km^2 in 2001, the built-up area expanded remarkably to 209.8 km^2 by 2014, representing an astonishing 111.1% increase. This exponential growth highlights the rapid transformation of the landscape, with built-up areas experiencing a notable surge in both size and density. Additionally, the study unveiled significant land conversions associated with urban expansion, notably the transformation of vegetated areas into bare land and built-up zones. Particularly noteworthy was the remarkable increase in the built-up area, expanding from 99.1 km^2 in 2001 to 121.8 km^2 in 2014, equivalent to a remarkable 122.9% total increase. This conversion underscores the dynamic nature of urban growth as vegetated landscapes yield to urban infrastructure and development.

The rapid urban expansion in Kaduna has led to significant land conversion, with

open spaces and designated industrial buffers being transformed into residential and commercial areas. This uncontrolled growth has resulted in the mixing of incompatible land uses, posing numerous risks to both the environment and public health [69]. Especially concerning are the risk areas identified around key industrial zones such as Kakuri industrial layout and KRPC refinery, including neighborhoods like Sabon Tasha, Jan Ruwa, Kamanzo, and Nasarawa. These areas are experiencing heightened levels of incompatible mixing, with industrial activities encroaching into residential and commercial spaces. This has elevated their risks and exposure to industrial effluents, emissions, and accidents for inhabitants, as well as environmental degradation due to the lack of proper buffer zones and infrastructure for waste management.

These findings necessitate urgent action from city authorities and urban planners to mitigate the risks associated with incompatible land use mixing. Strategic planning measures should be implemented to regulate urban expansion, protect designated industrial areas, and establish appropriate buffer zones to safeguard residential and commercial zones. Additionally, targeted interventions are needed to enhance infrastructure resilience and improve waste management practices in areas experiencing rapid urbanization.

Author contributions: Conceptualization, KMK; methodology, KMK; software, KMK; validation, SI, MAU and KHO; formal analysis, KMK; investigation, KMK and FUA; resources, KMK and SI; data curation, SI; writing—original draft preparation, KMK; writing—review and editing, SI, MAU and KHO; visualization, SI, FUA and KHO; project administration, KMK. All authors have read and agreed to the published version of the manuscript.

Conflict of interest: The authors declare no conflict of interest.

References

1. Billah M, Rahman GA. Land cover mapping of Khulna city applying remote sensing technique. Bangladesh University of Engineering and Technology. 2004; 2: 46–59.
2. Cui Y, Cheng D, Choi CE, et al. The cost of rapid and haphazard urbanization: lessons learned from the Freetown landslide disaster. Landslides. 2019; 16: 1167–76.
3. Unger E-M, Zevenbergen J, Bennett R, Lemmen C. Application of LADM for disaster prone areas and communities. Land Use Policy. 2019; 80: 118–26. doi: 10.1016/j.landusepol.2018.10.012
4. Kunwar S, Ferdush J. Mapping of Land Use and Land Cover (LULC) using EuroSAT and Transfer Learning. Revue Internationale de Geomatique. 2023; 33: 1-13.
5. Agbola T. Kaduna. Cities. 1986; 3: 282–289.
6. Abolade AO, Dugeri T, Adama JU. Challenges of digitalizing land administration system in Nigeria: The Kaduna State experience. In: Proceedings of the 18th African real estate society (AFRES) annual conference; 2018. pp. 67–82.
7. Sati S, Danwalis S. Analysis of Land Use Changes in Kaduna North Local Government Area, Nigeria. Ethiopian Journal of Environmental Studies & Management. 2020; 13: 126–37.
8. Liu J, Jiao L, Zhang B, Xu G, Yang L, Dong T, et al. New indices to capture the evolution characteristics of urban expansion structure and form. Ecological Indicators. 2021; 122: 107302.
9. Kasei RA, Kalanda-Joshua MD, Benefor DT. Rapid urbanisation and implications for indigenous knowledge in early warning on flood risk in African cities. Journal of the British Academy. 2019; 7: 183–214.
10. Kafi KM, Barau AS, Aliyu A. The effects of windstorm in African medium-sized cities: An analysis of the degree of damage using KDE hotspots and EF-scale matrix. International Journal of Disaster Risk Reduction. 2021; 55: 102070.

11. Ul Din S, Mak HWL. Retrieval of land-use/land cover change (LUCC) maps and urban expansion dynamics of Hyderabad, Pakistan via Landsat datasets and support vector machine framework. Remote Sensing. 2021; 13: 3337.
12. Shi H, Zhao M, Chi B. Behind the land use mix: Measuring the functional compatibility in urban and sub-urban areas of China. Land. 2021; 11: 2.
13. Beillouin D, Cardinael R, Berre D, et al. A global overview of studies about land management, land-use change, and climate change effects on soil organic carbon. Global Change Biology. 2022; 28: 1690–702. doi: 10.1111/gcb.15998.
14. Wu H, Shah SMA, Nawaz A, et al. Disaster management policy development and engineering economics: an analysis of game-changing impact of COVID 19 on oil-power industry, environment, and economy. Revista Argentina de Clínica Psicológica. 2020; 29: 550.
15. Jiang H, Sun Z, Guo H, Weng Q, Du W, Xing Q, et al. An assessment of urbanization sustainability in China between 1990 and 2015 using land use efficiency indicators. Npj Urban Sustainability. 2021; 1: 34.
16. Barau AS, Kafi KM, Mu'allim MA, Dallimer M, Hassan A. Comparative mapping of smellscape clusters and associated air quality in Kano City, Nigeria: An analysis of public perception, hotspots, and inclusive decision support tool. Sustainable Cities and Society. 2023; 96.
17. Sandström UG, Angelstam P, Khakee A. Urban comprehensive planning—identifying barriers for the maintenance of functional habitat networks. Landscape and Urban Planning. 2006; 75: 43–57. doi: 10.1016/j.landurbplan.2004.11.016
18. Steiner F. Frontiers in urban ecological design and planning research. Landscape and Urban Planning. 2014; 125: 304–11.
19. Zhao L, Li H, Sun Y, et al. Planning emergency shelters for urban disaster resilience: An integrated location-allocation modeling approach. Sustainability. 2017; 9: 2098.
20. Kafi KM, Shafri HZM, Shariff ABM. An analysis of LULC change detection using remotely sensed data; A Case study of Bauchi City. IOP Conf Ser: Earth Environ Sci. 2014; 20: 012056. doi: 10.1088/1755-1315/20/1/012056
21. Maddah S, Karimi S, Rezai H, Khaledi J. Detecting Land use Changes Affected by Human Activities using Remote Sensing (Case Study: Karkheh River Basin). Curr World Environ. 2015; 10: 473–81. doi: 10.12944/CWE.10.2.11
22. Panuju DR, Paull DJ, Griffin AL. Change detection techniques based on multispectral images for investigating land cover dynamics. Remote Sensing. 2020; 12: 1781.
23. Nkiruka EM, Chinedu AD, Smart UN. Landuse, landcover change dynamics and flooding in the lower Niger basin Onitsha, South Eastern Nigeria. Land Use Policy. 2023; 131: 106748. doi: 10.1016/j.landusepol.2023.106748
24. Aburas MM, Ho YM, Ramli MF, Ash'aari ZH. The simulation and prediction of spatio-temporal urban growth trends using cellular automata models: A review. International Journal of Applied Earth Observation and Geoinformation. 2016; 52: 380–9. doi: 10.1016/j.jag.2016.07.007
25. Wang J, Bretz M, Dewan MAA, Delavar MA. Machine learning in modelling land-use and land cover-change (LULCC): Current status, challenges and prospects. Science of The Total Environment. 2022; 822: 153559.
26. Hyandye CB, Worqul A, Martz LW, Muzuka ANN. The impact of future climate and land use/cover change on water resources in the Ndembera watershed and their mitigation and adaptation strategies. Environ Syst Res. 2018; 7: 7. doi: 10.1186/s40068-018-0110-4
27. Singh RK, Singh P, Drews M, Kumar P, Singh H, Gupta AK, et al. A machine learning-based classification of LANDSAT images to map land use and land cover of India. Remote Sensing Applications: Society and Environment. 2021; 24: 100624.
28. Giri C, Zhu Z, Reed B. A comparative analysis of the Global Land Cover 2000 and MODIS land cover data sets. Remote Sensing of Environment. 2005; 94: 123–32.
29. Agapiou A, Lysandrou V, Hadjimitsis DG. Earth observation contribution to cultural heritage disaster risk management: case study of Eastern Mediterranean open air archaeological monuments and sites. Remote Sensing. 2020; 12: 1330.
30. Mahamoud A, Maher G, Mohamed NA, et al. Monitoring shoreline change using remote sensing, GIS, and field surveys: a case study of the Ngazidja Island Coast, Comoros. Arab J Geosci. 2023; 16: 114. doi: 10.1007/s12517-023-11200-y
31. Roy DP, Lewis PE, Justice CO. Burned area mapping using multi-temporal moderate spatial resolution data—A bi-directional reflectance model-based expectation approach. Remote Sensing of Environment. 2002; 83: 263–86.
32. Mundia CN, Aniya M. Analysis of land use/cover changes and urban expansion of Nairobi city using remote sensing and GIS. International Journal of Remote Sensing. 2005; 26: 2831–2849. doi: 10.1080/01431160500117865
33. Piramanayagam S, Saber E, Schwartzkopf W, Koehler FW. Supervised classification of multisensor remotely sensed images using a deep learning framework. Remote Sensing. 2018; 10: 1429.
34. Ilunga JTW, Kalombo DK, Inabanza ON, et al. Contributions of Remote Sensing and GIS to the Inventory and Mapping of

Colonial Geodetic Markers in the Katangese Copper Belt. RIG. 2024; 33.
35. Isa Z, Sawa BA, Abdussalam AF, et al. Impact of climate change on climate extreme indices in Kaduna River basin, Nigeria. Environ Sci Pollut Res. 2023; 30: 77689–712. doi: 10.1007/s11356-023-27821-5
36. Bununu YA, Ludin ANM, Hosni N. City profile: Kaduna. Cities. 2015; 49: 53–65.
37. Ishaya S, Abaje IB. Indigenous people's perception on climate change and adaptation strategies in Jema'a local government area of Kaduna State, Nigeria. Journal of Geography and Regional Planning. 2008; 1: 138.
38. Al-Amin MA, Dadan-Garba A. Urban vegetation study of Kaduna Metropolis using GIS and remotely sensed data. Journal of Natural Sciences Research. 2014; 4: 160–71.
39. Bruce CM, Hilbert DW. Pre-processing methodology for application to Landsat TM/ETM+ imagery of the wet tropics. Cairns, Qld.: Rainforest CRC; 2006.
40. Yu Z, Di L, Yang R, Tang J, et al. Selection of landsat 8 OLI band combinations for land use and land cover classification. In: Proceedings of the 2019 8th International Conference on Agro-Geoinformatics (Agro-Geoinformatics); 2019. pp. 1–5.
41. Lock M. Kaduna, 1917, 1967, 2017: a survey and plan of the capital territory for the government of Northern Nigeria. (No Title). London: Faber and Faber; 1967.
42. Zhu Z. Change detection using landsat time series: A review of frequencies, preprocessing, algorithms, and applications. ISPRS Journal of Photogrammetry and Remote Sensing. 2017; 130: 370–84.
43. Yang X, Lo CP. Using a time series of satellite imagery to detect land use and land cover changes in the Atlanta, Georgia metropolitan area. International Journal of Remote Sensing. 2002; 23: 1775–98. doi: 10.1080/01431160110075802
44. Chen Z, Yang B, Wang B. A preprocessing method for hyperspectral target detection based on tensor principal component analysis. Remote Sensing. 2018; 10: 1033.
45. Barsi JA, Markham BL, Czapla-Myers JS, et al. Landsat-7 ETM+ radiometric calibration status. In: Proceedings of Spiethe International Society for Optical Engineering. NIH Public Access; 2016.
46. Chander G, Markham BL, Helder DL. Summary of current radiometric calibration coefficients for Landsat MSS, TM, ETM+, and EO-1 ALI sensors. Remote Sensing of Environment. 2009; 113: 893–903.
47. Alexandri G, Georgoulias AK, Meleti C, et al. A high resolution satellite view of surface solar radiation over the climatically sensitive region of Eastern Mediterranean. Atmospheric Research. 2017; 188: 107–21. doi: 10.1016/j.atmosres.2016.12.015
48. Jiang J, Zheng H, Ji X, et al. Analysis and evaluation of the image preprocessing process of a six-band multispectral camera mounted on an unmanned aerial vehicle for winter wheat monitoring. Sensors. 2019; 19: 747.
49. Horning N. Selecting the appropriate band combination for an RGB image using Landsat imagery. New York, USA; 2004.
50. Lillesand T, Kiefer RW, Chipman J. Remote sensing and image interpretation. John Wiley & Sons; 2015.
51. Foody GM, Mathur A, Sanchez-Hernandez C, Boyd DS. Training set size requirements for the classification of a specific class. Remote Sensing of Environment. 2006; 104: 1–14.
52. Benza M, Weeks JR, Stow DA, et al. A pattern-based definition of urban context using remote sensing and GIS. Remote Sensing of Environment. 2016; 183: 250–64. doi: 10.1016/j.rse.2016.06.011
53. Wu W, Chen WY, Yun Y, et al. Urban greenness, mixed land-use, and life satisfaction: Evidence from residential locations and workplace settings in Beijing. Landscape and Urban Planning. 2022; 224: 104428. doi: 10.1016/j.landurbplan.2022.104428
54. Momeni R, Aplin P, Boyd DS. Mapping complex urban land cover from spaceborne imagery: The influence of spatial resolution, spectral band set and classification approach. Remote Sensing. 2016; 8: 88.
55. Hilpert M. Setbacks for gas stations in a world with regionally varying emissions factors and acceptable health risks. Frontiers in Environmental Health. 2023; 2: 1214376.
56. Lewis C, Greiner LH, Brown DR. Setback distances for unconventional oil and gas development: Delphi study results. PLoS One. 2018; 13: e0202462.
57. Lü YL, Geng J, He GZ. Industrial transformation and green production to reduce environmental emissions: Taking cement industry as a case. Advances in Climate Change Research. 2015; 6: 202–9.
58. Mak HWL, Laughner JL, Fung JCH, et al. Improved satellite retrieval of tropospheric NO2 column density via updating of air mass factor (AMF): Case study of Southern China. Remote Sensing. 2018; 10: 1789.
59. Vural E. Assessment of Particle Matter Pollution during Post-Earthquake Debris Removal in Adiyaman City. Ridg. 2024; 33: 37–50. doi: 10.32604/rig.2024.047908
60. Usman MB, Sanusi YA, Musa D. Physical and commuting characteristics of selected peri-urban settlements in Kaduna,

Kaduna State, Nigeria. Journal of Geography and Regional Planning. 2017; 10: 317–29.
61. Kodag S, Mani SK, Balamurugan G, Bera S. Earthquake and flood resilience through spatial Planning in the complex urban system. Progress in Disaster Science. 2022; 14: 100219. doi: 10.1016/j.pdisas.2022.100219
62. Kafi KM, Ponrahono Z, Salisu Barau A. Addressing knowledge gaps on emerging issues in weather and climate extreme events: a systematic review. Climatic Change. 2024; 177: 56. doi: 10.1007/s10584-024-03714-5
63. Tini NH, Light BJ. Impacts of Urban Sprawl on Livability in Kaduna Metropolis, Nigeria. International Journal of Scientific Research in Science and Technology. 2020; 7: 334–43.
64. Siegan BH. Land use without zoning. Rowman & Littlefield Publishers; 2020.
65. Shi Q, Cao G. Urban spillover or rural industrialisation: Which drives the growth of Beijing Metropolitan Area. Cities. 2020; 105: 102354.
66. Barau AS. Transitioning to inclusive and nature-based decarbonisaton through recreating tree-based artisanal industries in Kano City, Nigeria. Norsk Geografisk Tidsskrift-Norwegian Journal of Geography. 2023: 1–12.
67. Adeyemi AA, Ojekunle ZO. Concentrations and health risk assessment of industrial heavy metals pollution in groundwater in Ogun state, Nigeria. Scientific African. 2021; 11: e00666.
68. Emigilati MA, Ishiaku I, Usman BY, et al. Assessment of effluents discharged from textiles industries in selected villages in Kaduna State, Nigeria. African Journal of Environmental Science and Technology. 2015; 9: 385–389.
69. Chi YL, Mak HWL. From comparative and statistical assessments of liveability and health conditions of districts in Hong Kong towards future city development. Sustainability. 2021; 13: 8781.
70. Jong P, Van Beek L. Spatial planning to improve the liveability of rural areas: a case from the Netherlands. In: AESOP Annual Congress proceedings. AESOP; 2024.